



## OPEN

SUBJECT AREAS:  
BIOLOGICAL SCIENCES  
DEVELOPMENTReceived  
11 July 2014Accepted  
17 September 2014Published  
10 October 2014Correspondence and  
requests for materials  
should be addressed to  
R.N. (ryusuke-niwa@  
umin.ac.jp)\* Current address:  
Biotechnology  
Research Center,  
Toyama Prefectural  
University, Imizu,  
Toyama 939-0398,  
Japan.

# A Halloween gene *noppera-bo* encodes a glutathione S-transferase essential for ecdysteroid biosynthesis via regulating the behaviour of cholesterol in *Drosophila*

Sora Enya<sup>1</sup>, Tomotsune Ameku<sup>1</sup>, Fumihiko Igarashi<sup>2\*</sup>, Masatoshi Iga<sup>2</sup>, Hiroshi Kataoka<sup>2</sup>, Tetsuro Shinoda<sup>3</sup> & Ryusuke Niwa<sup>1,4</sup>

<sup>1</sup>Graduate School of Life and Environmental Sciences, University of Tsukuba, Tennoudai 1-1-1, Tsukuba, Ibaraki 305-8572, Japan, <sup>2</sup>Department of Integrated Biosciences, Graduate School of Frontier Sciences, The University of Tokyo, Kashiwanoha 5-1-5, Kashiwa, Chiba 277-8562, Japan, <sup>3</sup>National Institute of Agrobiological Sciences, Owashi 1-2, Tsukuba, Ibaraki 305-8634, Japan, <sup>4</sup>PRESTO, Japan Science and Technology Agency, Honcho 4-1-8, Kawaguchi, Saitama 332-0012, Japan.

In insects, the precise timing of moulting and metamorphosis is strictly guided by ecdysteroids that are synthesised from dietary cholesterol in the prothoracic gland (PG). In the past decade, several ecdysteroidogenic enzymes, some of which are encoded by the Halloween genes, have been identified and characterised. Here, we report a novel Halloween gene, *noppera-bo* (*nobo*), that encodes a member of the glutathione S-transferase family. *nobo* was identified as a gene that is predominantly expressed in the PG of the fruit fly *Drosophila melanogaster*. We generated a *nobo* knock-out mutant, which displayed embryonic lethality and a naked cuticle structure. These phenotypes are typical for Halloween mutants showing embryonic ecdysteroid deficiency. In addition, the PG-specific *nobo* knock-down larvae displayed an arrested phenotype and reduced 20-hydroxyecdysone (20E) titres. Importantly, both embryonic and larval phenotypes were rescued by the administration of 20E or cholesterol. We also confirm that PG cells in *nobo* loss-of-function larvae abnormally accumulate cholesterol. Considering that cholesterol is the most upstream material for ecdysteroid biosynthesis in the PG, our results raise the possibility that *nobo* plays a crucial role in regulating the behaviour of cholesterol in steroid biosynthesis in insects.

Ecdysteroids, including ecdysone and its derivative 20-hydroxyecdysone (20E), are the principal insect steroid hormones that play pivotal roles in controlling a number of developmental and physiological events, especially moulting and metamorphosis<sup>1,2</sup>. During postembryonic development, ecdysone is synthesised from dietary sterols, such as cholesterol, via a series of hydroxylation and oxidation steps in an endocrine organ called the prothoracic gland (PG)<sup>3-5</sup>. Ecdysone is secreted in the haemolymph and subsequently converted to the more biologically active hormone 20E in peripheral tissues<sup>3</sup>.

In the past 15 years, a number of ecdysteroidogenic enzymes have been successfully identified and characterised, especially in the fruit fly, *Drosophila melanogaster* (See ref. 5 and references therein). Neverland (Nvd) is the [2Fe-2S] Rieske oxygenase and mediates the first step of the ecdysteroid biosynthesis pathway, which is the 7,8-dehydrogenation of cholesterol to 7-dehydrocholesterol (7dC). 7dC is then converted to 5 $\beta$ -ketodiol through the 'Black Box'. The 'Black Box' has not yet been biochemically characterised but is thought to be catalysed by at least 3 enzymes, including the cytochrome P450 monooxygenases Spook (Spo), CYP6T3 and the short-chain dehydrogenase/reductase Shroud (Sro). The conversion of 5 $\beta$ -ketodiol to 20E is catalysed by a series of cytochrome P450s: i.e., Phantom (Phm), Disembodied (Dib), Shadow (Sad) and Shade (Shd). In particular, *spo*, *sro*, *phm*, *dib*, *sad* and *shd* are known as Halloween genes, whose complete loss-of-function mutations result in typical embryonic cuticular differentiation defects<sup>5,6</sup>.

Currently, however, it has not been proved that these identified ecdysteroidogenic enzymes are sufficient to synthesise 20E from dietary sterols. Therefore, it is still possible that uncharacterised enzymes play an essential role in ecdysteroid biosynthesis by catalysing a known or unknown chemical reaction. To uncover an unidentified gene responsible for ecdysteroid biosynthesis, we have been conducting gene expression analyses to identify and characterise genes that are highly expressed in the PG<sup>7-13</sup>. Here, we report an additional gene responsible for



ecdysteroid biosynthesis in *D. melanogaster*, designated as *noppera-bo* (*nobo*), that encodes a glutathione S-transferase (GST). *nobo* and its orthologues are conserved in Diptera and Lepidoptera. *nobo* loss-of-function animals display a number of typical phenotypes caused by a low ecdysteroid titre. Finally, we show that loss-of-function of *nobo* causes abnormal accumulation of cholesterol in PG cells. We propose that *nobo* GST proteins are novel, indispensable regulators of ecdysteroid biosynthesis.

## Results

**The expression of the GST gene *CG4688* (*noppera-bo*) strongly correlates with ecdysteroid biosynthesis.** In the course of *D. melanogaster* microarray analysis to screen for genes predominantly expressed in the ring gland (RG), a composite endocrine organ containing the PG cells (T.S., unpublished data), we focused on a gene called *CG4688*, also known as *GSTe14*<sup>14</sup>. A quantitative reverse-transcription PCR analysis revealed that the spatial expression of *CG4688* was restricted to the ring gland (RG), a composite endocrine organ containing the PG cells, during larval development (Fig. 1a). *CG4688* expression was also weakly detected in the adult ovary that is known to synthesise ecdysone (Fig. 1a). *In situ* hybridisation and immunohistochemical analyses also confirmed that *CG4688* was predominantly expressed in the PG cells of the third (final) instar larval stages (Fig. 1b,c), as well as in ovarian follicle cells (Fig. 1d,e). The RG contains not only the PG but also other endocrine organs, the corpus allatum (CA) and the corpus cardiacum (CC). The *CG4688* transcript was exclusively observed in the PG but not in the CA or CC (Fig. 1b',c').

In *D. melanogaster*, the early embryonic expression of the Halloween genes is essential for ecdysteroid biosynthesis prior to the formation of the PG<sup>5,6</sup>. The embryonic expression pattern of *CG4688* correlated well with a change in the embryonic ecdysteroid titre<sup>15</sup>. While no or little maternal *CG4688* mRNA was detected, the maximum level of embryonic *CG4688* expression was observed at 2–6 hours after egg laying (AEL) (Fig. 1f), which roughly corresponds to embryonic stages 5–10 (Fig. 1g–j; also see Supplementary fig. S1 for sense probe). *CG4688* expression decreased in later embryogenesis (Fig. 1f). It should also be noted that the temporal expression fluctuation of *CG4688* is very similar to that of *shroud* (Fig. 1f), which was described previously<sup>16</sup>. We also conducted *in situ* RNA hybridisation analysis to examine *nobo* expression during embryogenesis. *nobo* was expressed in the blastoderm embryo with a ventral bias (Fig. 1g and Supplementary fig. S1a). As cellularisation proceeded, *nobo* expression was observed almost ubiquitously in the epidermal cells (Fig. 1h–j and Supplementary fig. S1b–d). In the germband elongation stage, *nobo* expression was up-regulated in the amnioserosa (Fig. 1k and Supplementary fig. S1e). At stage 16 and later, *nobo* expression was detected in the PG cells (Fig. 1l). This expression pattern is reminiscent of some Halloween genes, such as *phm* and *spo*<sup>7,17,18</sup>.

Previous studies have shown that expressions of most ecdysteroidogenic enzyme genes in the PG are positively control by prothoracicotropic hormone (PTTH) and its receptor Torso<sup>9,16,19–21</sup>. We found that *CG4688* expression was also significantly reduced in the third instar larvae of *ptth* neuron-ablated and *torso* RNA interference (RNAi) animals (Fig. 1m). All of these results demonstrate that *CG4688* expression is strongly correlated with ecdysteroid biosynthesis. Hereafter, we refer to *CG4688* as *noppera-bo* (*nobo*) for a reason explained later.

***Noppera-bo* is a Halloween gene.** Next, we assessed the functional importance of *nobo* *in vivo*. Previous studies have shown that six ecdysteroidogenic enzyme genes, *spo*, *sro*, *phm*, *dib*, *sad* and *shd*, belong to the Halloween group of mutants, which were originally identified in Nusslein-Volhard and Wieschaus' large saturated mutant screen and characterised by embryonic lethality and by

similar cuticular patterning<sup>5,6,22,23</sup>. While *nobo* is located at the 49F12 cytological position of the 2nd chromosome in *D. melanogaster*, there was no record of any typical Halloween mutants mapped in the vicinity of *nobo* in the previous screen<sup>22</sup>.

Thus, we created a null allele of *nobo* by a conventional knock-out technique<sup>24,25</sup>. In our *nobo* knock-out allele (*nobo*<sup>KO</sup>), an almost entire coding sequence region of *nobo* was replaced with a *mini-white* gene targeting cassette (Fig. 2a). Homozygotes of *nobo*<sup>KO</sup> were embryonic lethal and, like other Halloween mutants, did not produce a differentiated cuticle structure (Fig. 2b,c). We also found that *nobo*<sup>KO</sup> homozygotes displayed abnormal morphogenetic movements that involve the failure of head involution, defects in dorsal closure and abnormal gut looping (Fig. 2d–g). Moreover, the epidermal expression of both *IMP-E1* and *IMP-L1*, which are ecdysteroid-inducible genes, was greatly reduced or absent in *nobo*<sup>KO</sup> mutants (Fig. 2h–k). These phenotypic characteristics are very similar to the feature of Halloween mutants<sup>6,23</sup>. We also confirmed that the lethality and phenotype of *nobo*<sup>KO</sup> mutants were solely due to the loss of *nobo* function, as shown by the fact that the lethality was rescued by *nobo* transgene expression driven by *phm-GAL4#22* (Table 1).

We next determined whether the lethality of the *nobo*<sup>KO</sup> mutant was rescued by delivering 20E midway through embryogenesis. With control ethanol treatment, no *nobo*<sup>KO</sup> homozygous embryos developed into first instar larvae (Table 2). By contrast, with 100 μM 20E application, some *nobo*<sup>KO</sup> mutant embryos hatched into first instar larvae (Table 2), whereas the rescued animals died at the first instar larvae and did not grow into the second instar stage on a normal diet (100%; N=46). These results suggest that *nobo* is required for embryonic ecdysteroid biosynthesis and is indeed classified as a Halloween gene. On the basis of the Halloween-class naked cuticle phenotype, we named *CG4688* '*noppera-bo*' after a legendary Japanese faceless ghost.

***Noppera-bo* is also crucial for ecdysteroid biosynthesis during larval development.** To investigate the importance of *nobo* during *D. melanogaster* larval development, we examined the phenotypes of either the overexpression or the knockdown of the *nobo* gene in the PG using the GAL4/UAS system. In a wild-type background, the overexpression of *nobo* using any GAL4 lines that we tested had no visible effect on development (data not shown). To knock down *nobo*, we performed transgenic RNAi experiments<sup>26</sup> using a transgenic line carrying an inverted repeat construct corresponding to the *nobo* mRNA (*nobo-IR*) under the control of the UAS promoter. When the *UAS-nobo-IR* strains were crossed with the PG-specific driver *phm-GAL4*, the RNAi animals caused larval lethality. The larval lethality was observed with two independent *UAS-nobo-IR* constructs (see Methods), each of which targeted a different region of the *nobo* mRNA (data not shown). Hereafter, we refer to the animals in which the *nobo* RNAi was driven by *phm-GAL4#22* with *UAS-nobo-IR#40316* (see Methods) as '*nobo* RNAi animals' for simplicity.

The lethal phase for *nobo* RNAi animals was examined in more detail. In our experimental conditions, *nobo* RNAi animals exhibited a ~1% reduction in the level of the *nobo* mRNA at the first instar stage (Fig. 3a). *nobo* RNAi animals completed embryogenesis, hatched normally, and most *nobo* RNAi animals showed no apparent morphological or behavioural defects until 24 hours after egg laying (AEL), i.e., until the first instar larval stage (Fig. 3b,c). However, at ~48 hours AEL, *nobo* RNAi animals showed apparent growth arrest compared with control animals (Fig. 3b,d). At 72 hours AEL, while about half of control animals grew to the third instar larval stage (Fig. 3b,e), almost all *nobo* RNAi animals were the second instar larvae (Fig. 3c,e). At 144 hours AEL, the majority of control animals became pupae (Fig. 3b,f), but *nobo* RNAi animals were still at the second instar stage and gradually died (Fig. 3c,f). At 240 hours AEL, almost all control animals became adults (Fig. 3b). At this time point,

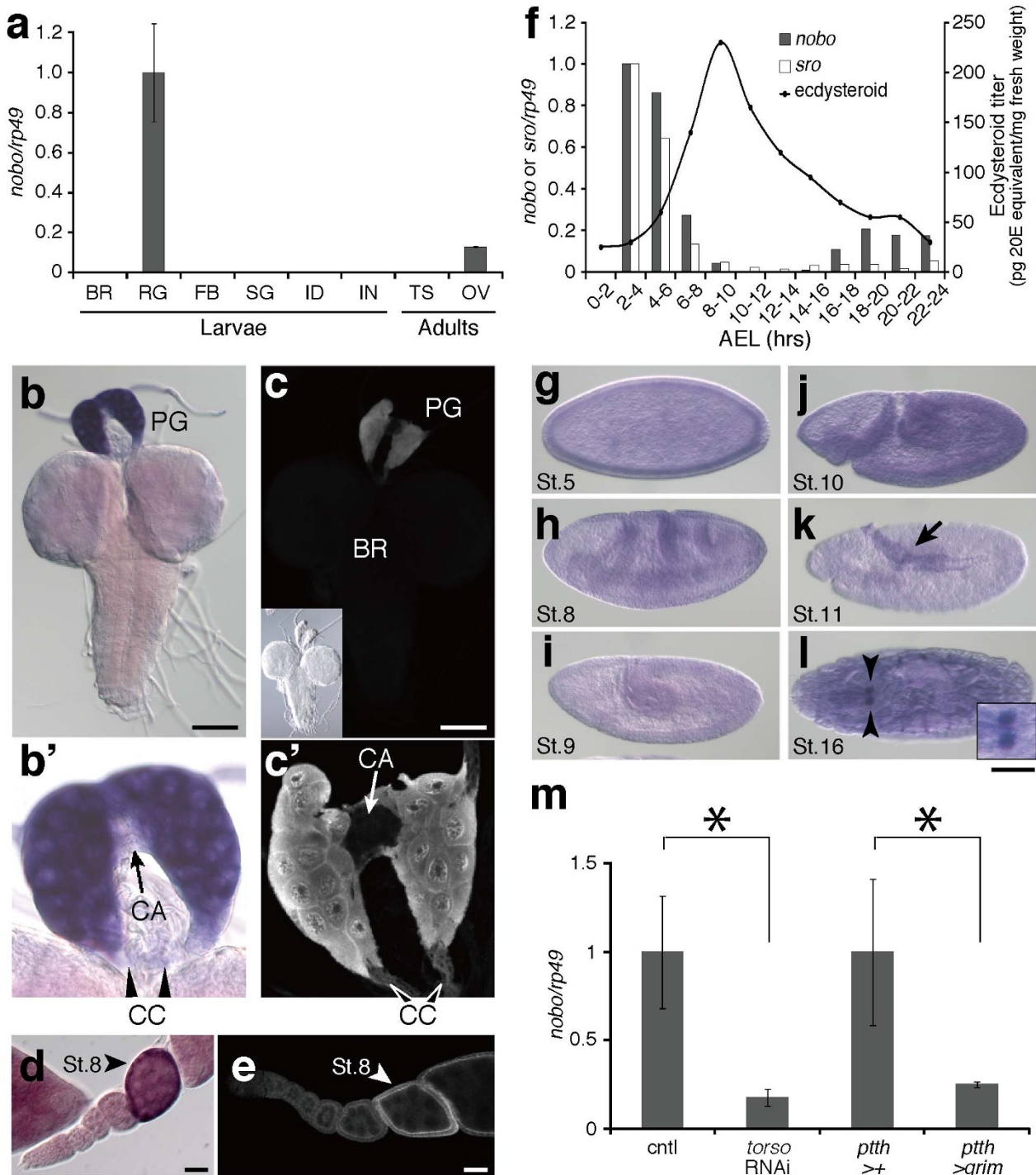


**Figure 1 | Expression pattern of *nobo*.** (a) The expression levels of *nobo* in several tissues were quantified by qRT-PCR. Total RNA samples were prepared from wandering third instar larvae and adult flies. BR, brain; RG, ring gland; FB, fat body; SG, salivary gland; ID, imaginal discs; IN, intestine; TS, adult testis; OV, adult ovary. Each error bar represents the s.e.m. from three independent samples. The normalised *nobo* mRNA level in the RG is set as 1. (b-e) Localisation of *nobo* mRNA and Nobo protein in the PG and the adult ovaries. (b, b') *In situ* signal with the *nobo* antisense RNA probe and (c, c') anti-Nobo immunoreactivity were detected in PG cells but not in other regions in the brain-ring gland complex of wandering third instar larvae. An inset of (c) shows a bright-field image of the same specimen. (b') and (c') show higher magnifications of the ring gland in (b) and (c), respectively. The arrow and arrowheads indicate the corpus allatum (CA) and the corpus cardiacum (CC), respectively. (d) *nobo* mRNA and (e) Nobo protein were strongly detected in the follicle cells of stage 8 (St.8) ovarioles in developing egg chambers. Scale bars: (b, c) 100  $\mu$ m, (d, e) 25  $\mu$ m. (f) The temporal expression profile of *nobo* during embryogenesis. A black line and white bars are schematic representations of the embryonic ecdysteroid titre and *sro* expression levels, respectively, based on published data<sup>15,16</sup>. The normalised *nobo* and *sro* mRNA levels at 2–4 hours AEL are set as 1. (g–l) *In situ* RNA hybridisation analysis in embryos with *nobo* antisense probe. Also see Supplementary fig. S1 for additional data. Lateral (g–k) and ventral (l) views are shown. (k) At stage 11 (St.11), the *nobo* signal was detected in the amnioserosa (arrow), which is thought to synthesise ecdysteroids. (l) At stage 16 (St.16), the *nobo* signal was detected in the PG cells (arrowheads). At this stage, a background staining in the epidermis was observed (Also see Supplementary fig. 1g). An inset with a higher magnification of the PG. Scale bar: 100  $\mu$ m. (m) qRT-PCR analysis of the *nobo* transcripts in the PGs isolated from 140  $\pm$  6 hour AEL third instar larvae of control, *torso* RNAi and *ptth*-expression neuron-ablated (*ptth*>*grim*) animals. Each error bar represents the s.e.m. from three independent samples. The *nobo* expression levels in each control were set as 1. \*,  $P < 0.05$  with Student's *t*-test.

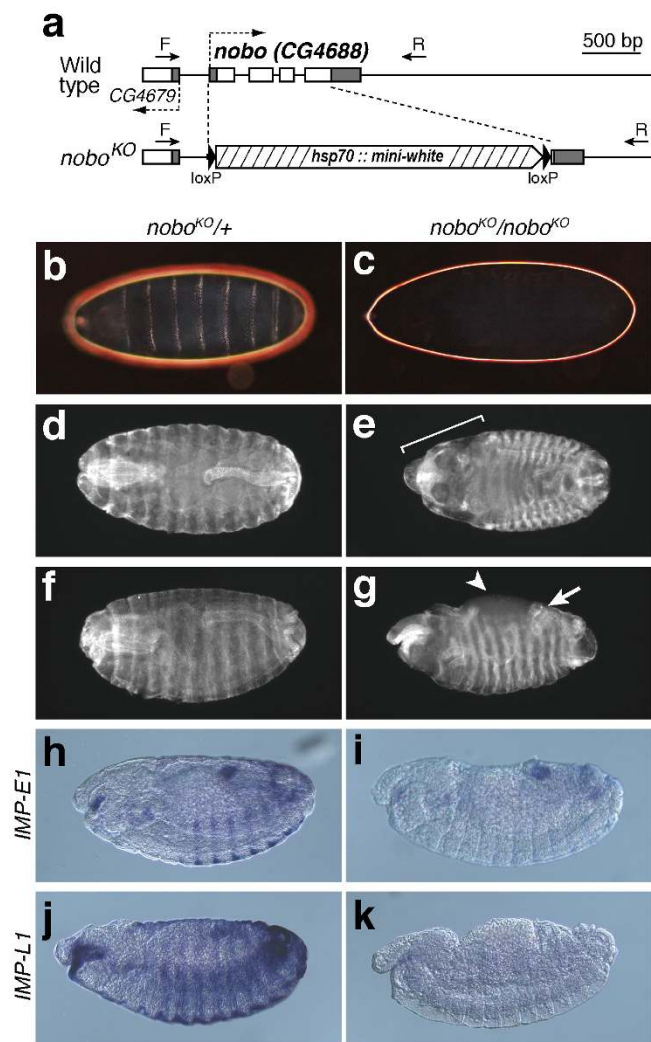


**Figure 2 | Generation and phenotypic analysis of *nobo*<sup>KO</sup> homozygous mutant embryos.** (a) Genomic and exon-intron structures of the *nobo* (CG4688) loci of the wild-type and *nobo* knock-out (*nobo*<sup>KO</sup>) strains. White and black boxes indicate the coding sequence and the untranslated regions, respectively. CG4649 is a gene located next to *nobo*. Dashed arrows indicate orientations of the genes. In the *nobo*<sup>KO</sup> allele, 1,033 bp of the *nobo* gene region was replaced with a gene-targeting construct including the *hsp70::mini-white* marker cassette with loxP sites, resulting in a 680 bp deletion in the entire (696 bp) *nobo* coding sequence. Arrows 'F' and 'R' indicate the positions of the genotyping primers used in Supplementary Fig. 2 (also see Methods and Supplementary table S3). (b,c) Dark-field images of embryonic cuticles from (b) *nobo*<sup>KO</sup> heterozygous (*nobo*<sup>KO/+</sup>) and (c) homozygous (*nobo*<sup>KO/nobo</sup><sup>KO</sup>) embryos. (d–g) Anti-FasIII antibody staining to visualise overall embryo morphology. (d,f) *nobo*<sup>KO/+</sup> embryos. (e, g) *nobo*<sup>KO/nobo</sup><sup>KO</sup> embryos. (e) The bracket indicates defective head involution. (g) The arrow and the arrowhead indicate the dorsal open phenotype and abnormal gut looping, respectively. (h–k) Expression patterns of (h, i) *IMP-E1* and (j, k) *IMP-L1* in stage 14 embryos. (h, j) *nobo*<sup>KO/+</sup> embryos. (i, k) *nobo*<sup>KO/nobo</sup><sup>KO</sup> embryos. These data show that the *nobo* mutant exhibited severe reductions of these 20E-inducible genes. Scale bars: 100  $\mu$ m for all images.

a majority of *nobo* RNAi animals had already died, and the few larvae that were still alive were arrested at the second instar larval stage (Fig. 3c).

We also confirmed that the larval lethality and larval arrest phenotype of *nobo* RNAi animals was due to the loss of ecdysteroids. We first examined ecdysteroid titre in the second instar larvae (60 hours

Table 1 | Viability of *nobo*<sup>KO</sup> and *nobo* RNAi animals with the expression of *nobo* and other GST genes. The number of viable *nobo*<sup>KO</sup>/*nobo*<sup>KO</sup> and *nobo* RNAi adults was scored. Transgenes were driven by *phm-GAL4#22* driver. Details of genetic crosses for this experiment are described in Supplemental table 1. Values in parentheses indicate the number of viable control non-*nobo*<sup>KO</sup> homozygous or non-RNAi progeny from the parental strains in the same experimental batches (see Supplemental table S1)

Background	Transgene	Number of adults
<i>nobo</i> <sup>KO</sup>	<i>nobo</i> #1	101 (220)
	<i>nobo</i> #2	124 (255)
	<i>nobo</i> #3	46 (102)
	<i>nobo</i> -Bm#1	85 (377)
	<i>nobo</i> -Bm#5	77 (348)
	CG6673B	0 (105)
	GSTe4	0 (102)
	GSTe12	0 (117)
	<i>nobo</i> RNAi	<i>nobo</i> -Bm#1
<i>nobo</i> -Bm#2		105 (350)
GSTe4		0 (92)
GSTe12		0 (105)
<i>Sepia</i>		0 (249)
CG6673A		0 (120)
CG6673B		0 (278)
CG6662		0 (107)

AEL) of control and *nobo* RNAi animals by mass-spectrometric analysis. In the control larvae, we detected  $1.55 \pm 0.27$  pg of 20 E/mg of wet weight (mean  $\pm$  s.e.m., N=5). In contrast, ecdysteroid titre in *nobo* RNAi animals (N=5) was below the quantifiable limit in the same experimental conditions (see Methods), suggesting that *nobo* RNAi impairs ecdysteroid biosynthesis during larval stages. Moreover, we also found that *nobo* RNAi animals fed yeast paste containing 20E just after hatching grew to the later larval, pupal and even adult stages (Fig. 4a, inset). These results demonstrate that, in addition to embryogenesis, *nobo* is also crucial for larval development via the regulation of ecdysteroid biosynthesis.

#### Administration of cholesterol rescues *noppera-bo* loss-of-function phenotypes.

To determine which step of ecdysteroid biosynthesis is affected by the loss of *nobo* function, we performed a feeding experiment with various precursors of 20E. If Nobo is involved in a certain ecdysteroid biosynthesis step, we expected that the larval arrest phenotype of the loss of *nobo* function animals would be rescued by an exogenous administration of intermediate(s) downstream of the biosynthesis step. We have applied the same logic to confirm the conversion steps of some ecdysteroidogenic enzymes, such as Sro<sup>16</sup> and Nvd<sup>11,27</sup>. Intriguingly, we found that *nobo*<sup>KO</sup> mutants were almost completely rescued and reached the first instar stage when their mothers were fed yeast paste supplemented with 0.5% (w/w) cholesterol or 7dC (Table 3). We confirmed the homozygosity of the rescued *nobo*<sup>KO</sup> first instar larvae by PCR

Table 2 | Rescue of homozygous *nobo*<sup>KO</sup> embryos by incubation with 20E. The numbers of the first instar larvae are indicated. Embryos of the indicated genotype were incubated with or without 100  $\mu$ M 20E. Genotypes were assessed by the presence of GFP signal

Steroid	Number of the 1st instar larvae	
	<i>nobo</i> <sup>KO</sup> / <i>nobo</i> <sup>KO</sup>	<i>nobo</i> <sup>KO</sup> /CyO Act-GFP
None	0	96
20E	64	145

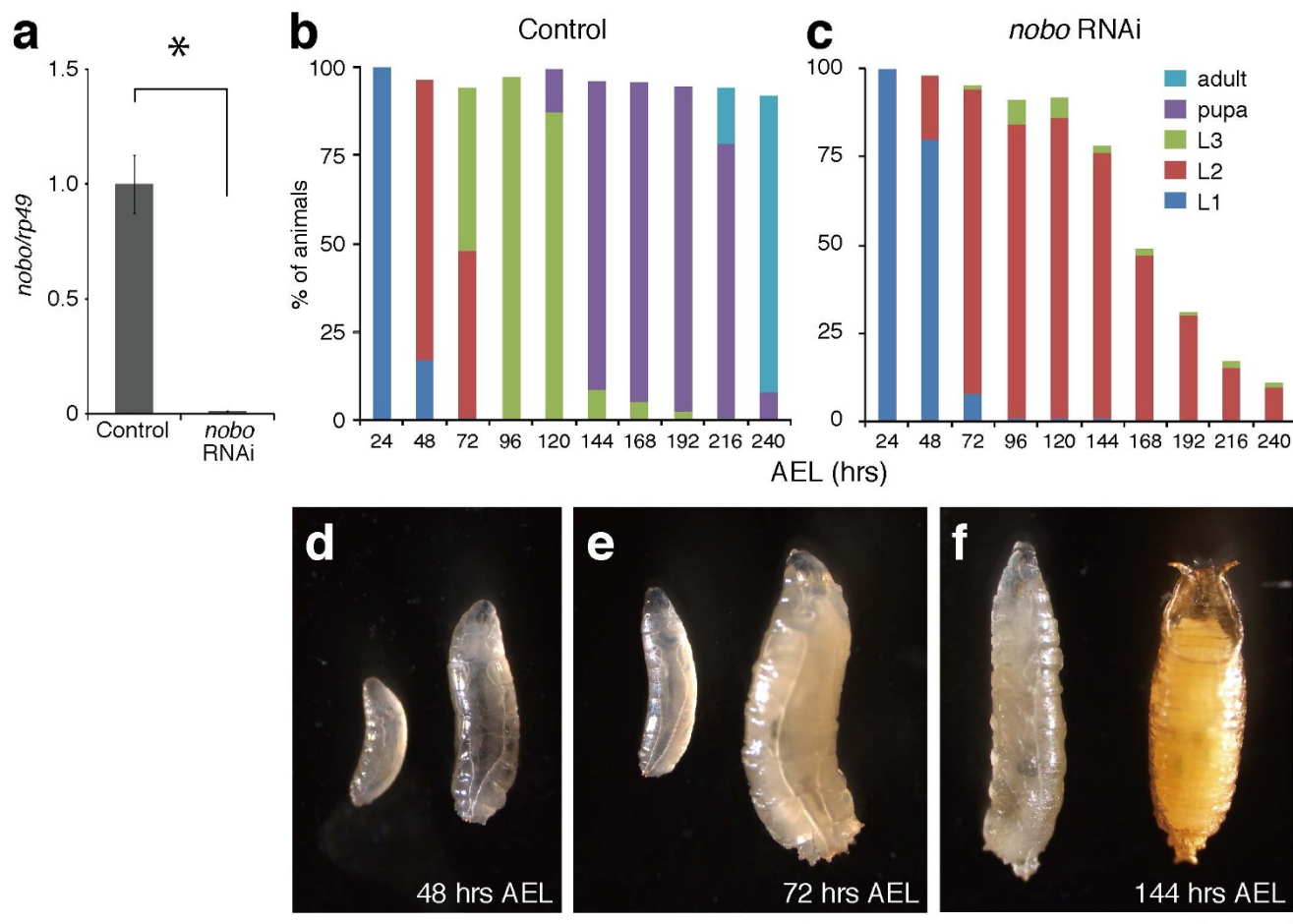


**Figure 3 | Larval lethality and developmental arrest phenotype of *nobo* RNAi larvae.** (a) Expression levels of control and *nobo* RNAi first instar larvae collected at 36 hours AEL. Each error bar represents the s.e.m. from three independent samples. The normalised *nobo* expression level in the control was set as 1. \*,  $P < 0.05$  with Student's *t*-test. (b,c) The survival rate and developmental progression of (b) control ( $N = 150$ ) and (c) *nobo* RNAi animals ( $N = 100$ ). L1, L2 and L3 indicate the first, second and third instar larvae, respectively. (d–f) Comparison of body size and developmental stage between control (right) and *nobo* RNAi (left) animals. Typically, control animals became the second instar larva, the third instar larva and pupa at (d) 48 hours (hrs), (e) 72 hours and (f) 144 hours AEL, respectively. In contrast, *nobo* RNAi animals in these photos are the first, second and second instar larvae, which were collected at each of the same time points, respectively. Scale bar: 1 mm.

genotyping (Supplementary fig. S2). Similarly, the *nobo* RNAi larvae on 0.5%(w/w) cholesterol- or 7dC-supplemented food moulted normally and grew into the adult stage (Fig. 4a). Considering the conventional view that cholesterol is the most upstream precursor of ecdysteroids in the PG<sup>3,28</sup>, these results suggest that *Nobo* may not convert identified ecdysteroid intermediates but may rather play a role in transport and/or metabolism in the PG.

We also examined the developmental phenotype of the homozygous *nobo*<sup>KO</sup> first instar larvae, which were derived by the maternal application of cholesterol described above. On a normal diet, all of the rescued *nobo*<sup>KO</sup> homozygous larvae exhibited a developmental arrest phenotype at the first or second instar larval stage, and none of them reached the third instar larval stage (Table 4). This larval arrest phenotype was due to ecdysteroid deficiency because the rescued *nobo*<sup>KO</sup> homozygous first instar larvae grew to the third instar larval stage on a diet supplemented with 20E (Table 4). In contrast to the RNAi animals, the larval arrest phenotype of the *nobo*<sup>KO</sup> larvae was not rescued when they were fed cholesterol- or 7dC-supplemented food (Table 4). These results suggest that the PG cells that completely lack *nobo* function cannot utilise cholesterol for ecdysteroid biosynthesis during larval development, whereas *nobo* RNAi PG cells, which are partial *nobo* loss-of-function cells, can. This point is argued in the Discussion below.

***Noppera-bo* plays a crucial role in cholesterol transport and/or metabolism.** We then examined whether cellular cholesterol in the PG cells was affected in *nobo* RNAi animals. A mass-spectrometric study revealed that the RG from the third instar larvae of conditional *nobo* RNAi significantly accumulated cholesterol compared to the RG from control animals (Fig. 4b). There were no statistically significant differences in the amounts of other plant and fungal sterols, contained in our regular diet such as  $\beta$ -sitosterol, ergosterol and campesterol, between control and *nobo* RNAi RG cells (Fig. 4b). We could not detect 7dC in either control or RNAi RG cells by our experimental method. To further confirm the abnormal accumulation of cholesterol, we dissected the RGs from the third instar larvae and incubated them *in vitro* with 22-NBD cholesterol, a fluorescent analogue of cholesterol<sup>29</sup>. We observed a significant elevation in fluorescence in the PG cells of *nobo* RNAi larvae compared to control animals (Fig. 4c,d). These results suggest that *Nobo* plays an essential role in the appropriate transport and/or metabolism of cholesterol for synthesising ecdysone.

**A subfamily of *noppera-bo* GST genes is well conserved in dipteran and lepidopteran species.** As classical phase II detoxification enzymes, GSTs are thought to have rapidly evolved in response to toxins and insecticides; thus, each insect genome encodes multiple

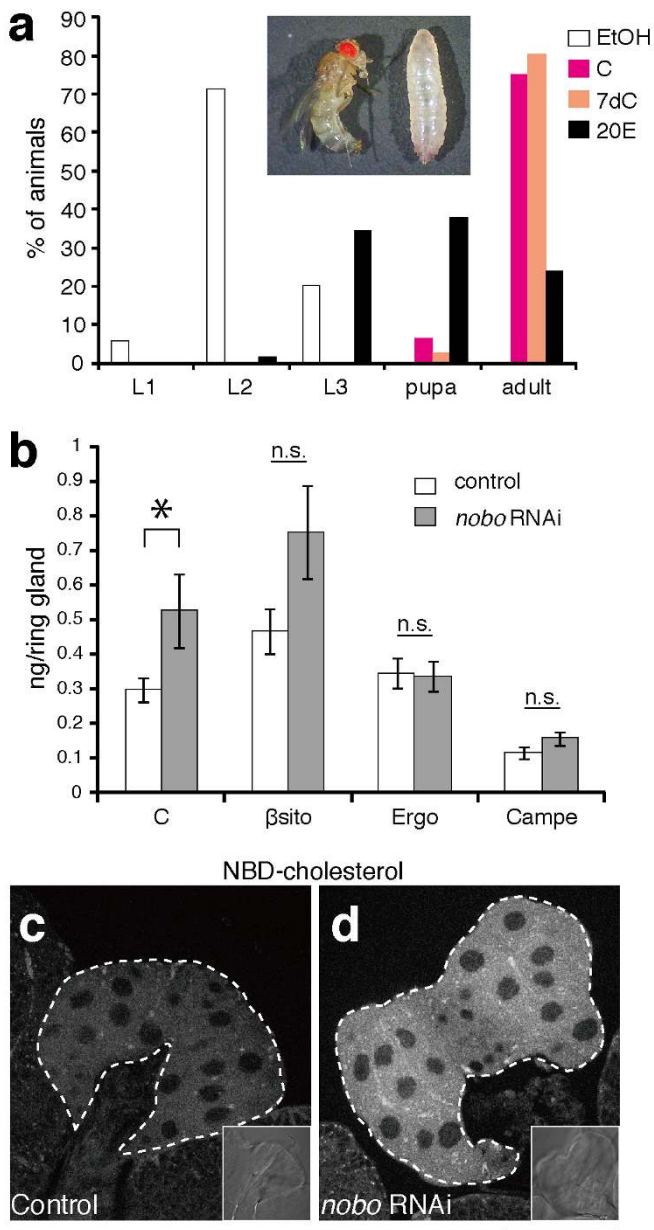


**Figure 4 | Feeding rescue experiments and abnormal cholesterol accumulation in *nobo* loss-of-function animals.** (a) Feeding rescue experiments for *nobo* RNAi larvae. *nobo* RNAi and control larvae were fed yeast paste supplemented with ethanol (EtOH, for negative control), cholesterol (C), 7-dehydrocholesterol (7dC) or 20E throughout their larval development. The concentration of each supplemented sterol in yeast paste was 0.5%(w/w) (See Methods for more details). The percentage of living animals at 240 hours AEL in each experimental condition was scored.  $N > 30$  for each experiments. Inset photo shows *nobo* RNAi animals at 240 hours AEL, which were raised on food with EtOH- (right) and 20E-supplemented (left) food, respectively. The larva (right) was at the 2nd instar stage. (b) Sterol amounts in the RG isolated from control and *nobo* RNAi larvae. C, cholesterol;  $\beta$ sito,  $\beta$ -sitosterol; Ergo, ergosterol; Campe, campesterol. 7dC amounts were under the detectable level in our experimental conditions, and thus, the 7dC data were not included in this graph.  $N = 10$  for each genotype. \*,  $P < 0.05$  with Student's *t*-test. n.s., not significant. Note that the higher level of  $\beta$ -sitosterol was observed in *nobo* RNAi PG cells, but the difference was not statistically significant. (c,d) Fluorescence and bright-field (inset) images of the PG from (c) control and (d) *nobo* RNAi animals incubated with 22-NBD-cholesterol. White dotted lines indicate the PG area. Scale bar: 50  $\mu$ m.

**Table 3 | Rescue of homozygous *nobo*<sup>KO</sup> embryos by maternal sterol administration.** The numbers of the first instar larvae that were offspring of *nobo*<sup>KO</sup>/CyO Act-GFP mothers, which were fed standard cornmeal food with yeast pastes containing 0.5%(w/w) each sterol, are indicated. Genotype was assessed by the presence of a GFP signal and genomic PCR results (See Supplementary fig. S2)

Sterol	Number of first instar larvae	
	<i>nobo</i> <sup>KO</sup> / <i>nobo</i> <sup>KO</sup>	<i>nobo</i> <sup>KO</sup> /CyO Act-GFP
None	0	44
C	79	129
7dC	63	118

GST genes<sup>30</sup>. *nobo* is found in the genomes of not only *D. melanogaster* but also other species of the genus *Drosophila*<sup>31</sup>. We further examined the evolutionarily conservation of *nobo* by analysing the phylogenetic relationship among *Nobo* and the other 277 GST proteins from 12 insects, the nematode *Caenorhabditis elegans* and *Homo sapiens* (Supplementary fig. 3a). *Nobo* belongs to the epsilon subclass, one of the six subclasses of insect cytosolic GSTs<sup>14</sup>. In the epsilon cluster, our phylogenetic analysis revealed that *D. melanogaster* *Nobo* is included in an evolutionarily conserved subclade, which also includes GSTs from dipteran species other than *Drosophilidae* species, such as the mosquitoes *Aedes aegypti*, *Anopheles gambiae*, and *Culex quinquefasciatus*, as well as lepidopteran species, such as the silkworm *Bombyx mori* and the monarch butterfly *Danaus plexippus* (Supplementary fig. 3a,b). The orthologous relationships between *A. gambiae*, *B. mori* and *D. melanogaster* are consistent with previous studies<sup>32,33</sup>. This conservation feature is in contrast to many other cytosolic GSTs, which are duplicated within a certain species (Supplementary fig. 3a). On the other hand, no clear orthologs of *nobo* were found in other insects than dipteran and lepidopteran species. These results suggest that *nobo* is evolutionarily conserved in Diptera and Lepidoptera.

According to the current GST nomenclature system, the orthologues of *nobo* from *D. melanogaster*, *A. gambiae* and *B. mori* are designated as GSTe14<sup>14</sup>, GSTe8<sup>32</sup> and GSTe7<sup>33</sup>, respectively. As described later, we succeeded in demonstrating that *B. mori* GSTe7 was functionally orthologous to *D. melanogaster* *nobo*. To avoid the further confusing numberings to represent the same functional orthologues among insect species, we would like to propose a unique subfamily name, *noppera-bo* (*nobo*), for these orthologues. Hereafter, we refer to *B. mori* GSTe7 as *nobo-Bm* in this manuscript.

**Table 4 | Rescue of homozygous *nobo*<sup>KO</sup> larvae by oral sterol administration.** The numbers of the first, second and third instar larvae of the *nobo*<sup>KO</sup> homozygous larvae, which were fed standard cornmeal food with yeast pastes containing 0.5%(w/w) sterol/sterol supplement, are indicated. Homozygous *nobo*<sup>KO</sup> larvae were obtained by maternal administration of cholesterol to homozygous *nobo*<sup>KO</sup> embryos as shown in Table 3. Larval instars were scored at 72 hours AEL

Sterol/steroid	Larval instar		
	First	Second	Third
None	16	2	0
C	18	4	1
7dC	18	6	0
20E	1	4	19



For the phylogenetic analysis, we also included human GSTA subclass members because previous studies have reported that some GSTA proteins are involved in steroidogenesis in mammals<sup>34–37</sup>. We found that the mammalian GSTA proteins were clustered in a clade completely different from the *Noppera-bo* subclade (Supplementary fig. 3a).

***Noppera-bo* GSTs play a conserved and specific role in insects.** To examine whether other insect orthologues of *nobo* also play conserved roles in ecdysteroid biosynthesis, we investigated whether the *nobo* gene from the silkworm *B. mori* (*nobo-Bm*) can compensate for *D. melanogaster nobo* loss-of-function during development. Indeed, the *phm-GAL4*-driven expression of *nobo-Bm* allowed both *nobo*<sup>KO</sup> homozygous mutants and *nobo* RNAi animals to complete their development and grow to adult stages (Table 1, Supplementary table S1 and S2). These results suggest that the *nobo* genes are truly functionally orthologous between Diptera and Lepidoptera. These data also confirm that the effect of the RNAi was specific to *nobo* and was not an off-target effect.

We further utilised the overexpression system to examine the functional specificity of *nobo* among other GST genes. A BLAST search indicated that the *nobo* gene is most similar to two epsilon-class GSTs in *D. melanogaster*, *GSTe4* and *GSTe12*. However, overexpression of neither *GSTe4* nor *GSTe12* could rescue the lethality of *nobo* loss-of-function animals (Table 1). We also obtained previously reported transgenic lines to overexpress other *D. melanogaster* GST genes, including *sepia*, *CG6662*, *CG6673A* and *CG6673B*<sup>38</sup>. In particular, *Sepia* and *CG6673A* are known to be involved in eye pigment synthesis and a neurodegeneration process, respectively, and their substrates have already been identified<sup>38,39</sup>. However, the overexpression of none of these genes rescued the lethality of *nobo* loss-of-function animals (Table 1). These results support the idea that *nobo* GSTs plays a unique role in controlling ecdysteroid biosynthesis.

## Discussion

In this study, we identified the *noppera-bo* (*nobo*) subfamily of GST proteins as components of the ecdysteroid biosynthetic pathway. All of our results indicate that *Nobo* plays a crucial role in ecdysteroid biosynthesis in *Drosophila melanogaster*. It is worth noting that a role of *D. melanogaster nobo* (*GSTe14*) in ecdysteroid biosynthesis has been independently demonstrated by Payre, Kageyama and their colleagues<sup>40</sup>.

GSTs are enzymes that conjugate the reduced form of glutathione (GSH) to various substrates. In general, GSTs are best known as cellular Phase II metabolic enzymes that catalyse the conjugation of GSH to xenobiotic substrates, including pollutants and drugs, for the purpose of detoxification in eukaryotes because GSH-conjugated substrates are easily transported out of cells<sup>41,42</sup>. In insects, GSTs are also essential for detoxifying endogenous and exogenous compounds. In particular, interest in insect GSTs has focused on their role in insecticide resistance<sup>43</sup> and phytochemical detoxification<sup>44,45</sup>.

However, in addition to the role in detoxification processes, some GSTs have indispensable functions in other essential cellular processes, such as the regulation of cellular signal transduction cascades and the production of essential metabolites in insects<sup>38,39</sup> and vertebrates<sup>46,47</sup>. In particular, previous studies have reported that the human GST A3-3 and its counterparts in other mammals are involved in mammalian steroid hormone biosynthesis<sup>34–37,48</sup>. Human GST A3-3 is selectively expressed in steroidogenic organs and catalyses the isomerisation of the  $\Delta^5$ -ketosteroid precursor in the biosynthesis of progesterone and testosterone. In conjunction with the studies in mammals, our study raises an interesting possibility that, similar to the families of cytochrome P450s and short-chain dehydrogenase/reductases<sup>5</sup>, the GST family is also involved in steroid hormone biosynthesis across animal phyla. It would be intriguing to

examine whether the steroid hormone biosynthesis pathways in other eukaryotes require GST proteins.

This study provides several lines of genetic evidence showing that *Nobo* is required for ecdysteroid biosynthesis via the regulation of cholesterol transport and/or metabolism. First, *nobo* is exclusively expressed in ecdysteroid-producing organs including the PG and the ovary. Second, *nobo*<sup>KO</sup> mutants exhibit a typical Halloween-class embryonic phenotype. Third, the larval developmental arrest phenotype is caused by the PG-specific knockdown of *nobo*. Finally, administration of 20E or cholesterol rescues *nobo* loss-of-function animals. However, compared to the known ecdysteroidogenic enzymes, *Nobo* is unique because *Nobo* seems not to be involved in the conversion of canonical ecdysteroid intermediates but to regulate the dynamics of cholesterol, which is normally thought to be the most upstream precursor of ecdysteroid biosynthesis. As far as we know, this is the first report suggesting that the behaviour of cholesterol in ecdysteroid biosynthesis is controlled by a specific factor whose expression and function are restricted to the ecdysteroidogenic organs.

As insects are unable to synthesize cholesterol *de novo*<sup>49</sup>, the increased cholesterol in *nobo* RNAi PG suggests that uptake of extracellular cholesterol, or intracellular transport and/or metabolism of cholesterol could be disordered in the PG. Using a fluorescent analogue of cholesterol, we observed a significant elevation in fluorescence in the PG cells of *nobo* RNAi larvae compared to control animals (Fig. 4c,d). This result raises two possibilities for *Nobo* function in wild-type PG: (1) *Nobo* inhibits the uptake of extracellular cholesterol in wild-type cells and thus may negatively regulate ecdysteroid biosynthesis or (2) *Nobo* is required for consumption of cholesterol via controlling transport and/or metabolism of intracellular cholesterol and thus may positively regulate ecdysteroid biosynthesis. Whereas we cannot completely rule out either of these possibilities, it appears the latter possibility is more likely because all of our genetic data strongly suggest that *nobo* is a positive regulator for promoting ecdysteroid biosynthesis. Related to this point, the loss-of-function phenotype of *nobo* is significantly similar to that of *Niemann-Pick type C disease-1a* (*NPC1a*)<sup>50–52</sup>, whose mammalian orthologues are essential for intracellular transport of cholesterol<sup>53</sup>. The shared phenotypic characteristics include the larval arrest phenotype due to the low ecdysteroid titre, the aberrant accumulation of sterols and the fact that the phenotype is rescued by dietary application of cholesterol and 7dC<sup>50–52</sup>. This consistency also supports our hypothesis that *Nobo* controls ecdysteroid biosynthesis by regulating the behaviour of intracellular cholesterol in the PG.

Our data show that the embryonic phenotype of *nobo*<sup>KO</sup> homozygotes is rescued by maternal application of cholesterol, whereas the larval arrest phenotype of the rescued *nobo*<sup>KO</sup> homozygote larvae is not rescued by oral cholesterol administration. We propose that these two phenomena are not paradoxical. In insects including *D. melanogaster*, the earlier embryonic stage of development is the syncytial stage, where an embryo possesses multiple nuclei without complete cell membranes in a single cytoplasm. Thus, maternally loaded excessive cholesterol can penetrate throughout the syncytial cytoplasm, resulting in the penetration of cholesterol throughout the blastodermal cells after cellularisation, even without *Nobo* function. In contrast, the larval PG cells take up cholesterol extracellularly and, thus, require *Nobo* to transport and/or metabolise this cholesterol. Therefore, unlike the embryos, *nobo*<sup>KO</sup> homozygote larvae cannot become final instar larvae even when they are fed cholesterol-supplemented food. If this scenario is correct, however, it actually raises another question: what endogenous sterol/steroidal precursor is transported and/or metabolised by *Nobo* for embryonic ecdysteroid biosynthesis in wild-type embryos. Currently, reliable precursor materials for embryonic ecdysteroids have not been reported.

It is actually puzzling that exogenously applied cholesterol can rescue the developmental arrest phenotype of the loss of *nobo* func-



tion animals even though cellular cholesterol abnormally accumulates. One speculation is that most endogenous cellular cholesterol might be somehow sequestered in an ‘unavailable’ form in loss of *nobo* function animals. This would be consistent with the accumulation and explain the reason why the administration of exogenous ‘available’ cholesterol rescues the *nobo* RNAi phenotype. Currently it remains to be delineated why cholesterol is accumulated in the loss of *nobo* function PG cells. To clarify this point, identifying substrate(s) of Nobo and pathway(s) affected by Nobo is obviously important.

Thus far, we have not been able to find a specific substrate for Nobo. Considering the differences in the chemical structures of steroid hormones and their biosynthesis pathways in mammals and insects, it is unlikely that Nobo catalyses the isomerisation of steroidal substrates as human GST A3-3 does. The only hint regarding the substrate(s) of Nobo from the transgenic rescue experiments using several types GST proteins (Table 1) is that Nobo might have a relatively narrow substrate specificity. One possibility is that Nobo conjugates GSH directly to small bioactive compound(s), such as cholesterol and/or other lipids to modulate the ecdysteroid biosynthesis pathway by an unknown mechanism. In the plant *Arabidopsis thaliana*, 12-oxo-phytodienoic acid (OPDA), the precursor of jasmonic acid, is conjugated with GSH, which is important for the transportation of OPDA into the vacuole<sup>54</sup>. By way of analogy to the observation in *Arabidopsis*, sterol-GSH conjugates may be necessary for a proper subcellular localisation and utilisation of sterols in the PG. An alternative possibility is that Nobo might conjugate GSH to a protein substrate that is essential for the behaviour of cholesterol transport and/or metabolism. In mammals, a growing amount of evidence suggests that glutathionylation of certain proteins is essential for modulating their functions in cells<sup>47</sup>. Previous studies have identified some essential proteins for regulating cholesterol metabolism and homeostasis in *D. melanogaster*<sup>28,55</sup>, including NPC1a. It is therefore worth examining whether Nobo conjugates GSH to these known regulators and modulates their functions in cholesterol metabolism.

Our phylogenetic analysis indicates that the *nobo* subfamily of GST proteins is well conserved in Diptera and Lepidoptera. We also demonstrate that the *in vivo* function of *D. melanogaster nobo* can be replaced with *B. mori nobo* (*nobo-Bm*), suggesting the functional orthologous relationship of *nobo* between Diptera and Lepidoptera. However, we could not find any clear orthologues of *nobo* in any other insect taxons (Supplementary fig. 3a). Because the GST family has great intra- and interspecies functional and structural diversity, it is possible that a simple BLAST search strategy and the neighbour-joining method failed to discover the true “functional” GST orthologues in other insect species. Alternatively, our data also raise the possibility that ecdysteroid biosynthesis is differentially regulated among insect species. Curiously, the essential ecdysteroidogenic enzyme genes *spookier* and *Cyp6t3* have so far only been found in the genomes of Drosophilidae<sup>18,56</sup>. In the future, it would be very interesting to study not only the evolutionary conservation of ecdysteroidogenic enzymes in arthropods<sup>57,58</sup> but also the specific molecular mechanisms of ecdysteroid biosynthesis in certain insects.

## Methods

**Fly strains.** *Drosophila melanogaster* flies were reared on standard agar-cornmeal medium at 25°C under a 12 h/12 h light/dark cycle. Oregon R was used as the wild-type strain for the *in situ* RNA hybridisation and immunohistochemistry shown in Fig. 1, and *w*<sup>1118</sup> was used as the wild-type (control) strain for all genetic experiments. The *UAS-nobo-IR* (stock numbers #40316 and #101884) and *UAS-torso-IR* (stock number #101154) strains were obtained from the Vienna *Drosophila* RNAi Center. *yw; P{CaryP}attP40<sup>59</sup>* was obtained from BestGene, Inc. *ptth-GAL4;UAS-grim*, in which the *ptth* gene-expressing neurons were ablated<sup>20</sup>, *phm-GAL4#22<sup>20,56</sup>* and *UAS-dicer2* were kindly gifted by M. B. O’Connor (University of Minnesota, USA). *UAS-sepia*, *UAS-CG6673A*, *UAS-CG6673B* and *UAS-CG6662<sup>38</sup>* were kind gifts from J. Yim (National University Seoul, Korea). *yw; P{70FLP}23 P{70I-SceI}4A/TM6<sup>24</sup> and w; P{70FLP}10<sup>24</sup>* were obtained from the Bloomington *Drosophila* Stock Center.

**Quantitative reverse transcription (qRT)-PCR.** Total RNA was isolated using the RNAsiso Plus reagent (TaKaRa). Genomic DNA was digested using Recombinant DNaseI (TaKaRa). cDNA was synthesised using the ReverTra Ace qRT RT Kit (TOYOBO). qRT-PCR was performed using the THUNDERBIRD SYBR qPCR Mix (TOYOBO) with a Thermal Cycler Dice TP800 system (TaKaRa). Serial dilutions of a plasmid containing the ORF of each gene were used as a standard. The expression levels were normalised to *rp49* in the same sample. The primers for quantifying *D. melanogaster nobo* are described in Supplementary table S3. Primers amplifying *rp49* were previously described<sup>60</sup>.

***in situ* RNA hybridisation.** To generate a template for synthesising sense and antisense *nobo* RNA probes, the *nobo* ORF region was isolated from the pUAST-*nobo-HA* vector (described below) and inserted into pBluescriptII digested with *EcoRI* and *NotI*, whose sites are positioned in the multicloning site of the pUAST-HA vector. Plasmids for synthesising the *IMP-E1* and *IMP-L1* probes have been previously described<sup>7</sup>. Synthesis of DIG-labelled RNA probes and *in situ* hybridisation were performed as previously described<sup>7</sup>.

**Generation of anti-Nobo antibody and immunohistochemistry.** Antibodies against the Nobo protein were raised in guinea pig. A synthetic peptide (NH<sub>2</sub>-MSQPKILYDDERSPPVRS-COOH) corresponding to residues 1–20 of the Nobo amino acid sequence (GenBank accession number AAF58397) was used for immunisation. Immunostaining for embryos, the brain-ring gland complex in third instar larvae and the ovary in female adults was performed as previously described<sup>7,61</sup>. The antibodies used were anti-Nobo antiserum (1 : 200 dilution), anti-FasIII 7G10 (obtained from the Developmental Studies Hybridoma Bank, Univ. of Iowa; 1 : 20 dilution), anti-guinea pig IgG antibody conjugated with Alexa488 (Life Technologies; 1 : 200 dilution), and anti-mouse IgG antibody conjugated with Alexa488 (Life Technologies; 1 : 200 dilution).

**UAS vectors, overexpression of genes and generation of transgenic strains.** The GAL4/UAS system<sup>62</sup> was used to overexpress genes in *D. melanogaster*. To generate pUAST vectors to overexpress *nobo* and *nobo-Bm* (*B. mori GSTe7*), specific primers (Supplementary table S3) were used for PCR to add *Bgl*III and *NotI* sites to the 5’ and 3’ ends, respectively, of each of the cDNA fragments corresponding to CDSs. Template cDNAs were reverse transcribed using total RNAs of the ring gland from *D. melanogaster* and the PG from *B. mori* (KINSHU x SHOWA F<sub>1</sub> hybrid) using Prime Script Reverse Transcriptase (TaKaRa). PCR was performed using Prime Star HS DNA polymerase (TaKaRa). The amplified CDS regions of *nobo* and *nobo-Bm* were digested with *Bgl*III and *NotI*, and then ligated into a pUAST-HA vector carrying a sequence coding three tandem HA tags at the C terminal<sup>7</sup>. To generate overexpression vectors of *GSTe12* and *GSTe4*, each CDS region was ligated into the pWALIU10-moe vector (purchased from Harvard RNAi Center; <http://www.flyrnai.org/TRiP-HOME.html>). Specific primers (Supplementary table S3) were used for PCR to add *Bgl*III and *Xba*I sites to the 5’ and 3’ ends, respectively, of each of the cDNA fragments corresponding to CDSs. Transformants were generated using the phiC31 integrase system in the *P{CaryP}attP40* strain. The *w*<sup>+</sup> transformants of pUAST and pWALIU10-moe were established using standard protocols.

**Generation of the gene-targeted *nobo*<sup>KO</sup> allele.** Gene-targeting of *nobo* was carried out by the ends-out method<sup>24,25</sup> using the pP{EndsOut2} and pBSII-70w<sup>63</sup> vectors provided by the Drosophila Genomics Resource Center and Dr. T. Matsuo (Tokyo Metropolitan Univ.), respectively. 5’ upstream and 3’ downstream regions of *nobo* were amplified by PCR with specific primer pairs (Supplementary table S3). Both PCR fragments were subcloned into pP{EndsOut2} with a *hsp70-white* mini-gene fragment excised from the pBSII-70w with *NotI* and *Hind*III. The *nobo* targeting vector was injected into the *w*<sup>+</sup> strain using standard protocols. Targeting crosses were carried out as described by the Sekelsky Lab (<http://sekelsky.bio.unc.edu/Research/Targeting/Targeting.html>). The *nobo* knock-out strain was back-crossed to the *w*<sup>1118</sup> strain for five generations.

**Embryonic cuticle preparation.** Embryonic cuticle preparation was carried out as previously described<sup>64</sup>.

**20E rescue of *nobo*<sup>KO</sup> embryos.** The 20E rescue experiment was performed as previously described<sup>16,18</sup>. 20E was purchased from Sigma. Homozygous *nobo*<sup>KO</sup> (*nobo*<sup>KO</sup>/*nobo*<sup>KO</sup>) embryos were obtained as offspring from *nobo*<sup>KO</sup>/CyO *Act5C-GFP* parents. Homozygous *nobo*<sup>KO</sup>/*nobo*<sup>KO</sup> embryos were distinguished from heterozygous *nobo*<sup>KO</sup> (*nobo*<sup>KO</sup>/CyO *Act5C-GFP*) embryos by assessing the presence or absence of a GFP signal under a fluorescence dissection microscope (Leica MZFLIII).

**Rescue experiments with ecdysteroid intermediates.** Cholesterol and 7-dehydrocholesterol (7dC) were purchased from Wako and Sigma, respectively. For maternal sterol rescue experiments, we used a *nobo*<sup>KO</sup> strain balanced with the CyO *Act5C-GFP* balancer chromosome, which carries a GFP expression construct. Female flies were kept on standard cornmeal food with yeast pastes containing 0.5% (w/w) sterol in 3.3% (w/w) ethanol (50 mg of yeast paste, 0.75 mg of sterol, 95 μl of water and 5 μl of ethanol) for 3 days. Then female flies were crossed with male flies of the same strain, which were reared on standard cornmeal food without steroidal supplement, and were left to lay eggs on grape agar plates for 1 day. At 24 hours AEL, the genotype of each hatched larva was scored by assessing the presence or absence of a GFP signal under a fluorescence dissection microscope MZFLIII (Leica). The





*nobo*<sup>KO</sup> allele was also distinguished from its wild-type sequence by genomic PCR with a specific primer pair (Fig. 2a and Supplementary table S3). Feeding rescue experiments for rescued *nobo*<sup>KO</sup> and *nobo* RNAi larvae were conducted as previously described<sup>11,16</sup>.

**Transgenic RNAi experiment and scoring of developmental progression.** *UAS-nobo-IR* and *w<sup>1118</sup>* flies were crossed with *UAS-dicer2*; *UAS-phm-GAL4#22* flies. Eggs were laid on grape plates with yeast pastes at 25°C for 4 hours. Fifty hatched first instar larvae were transferred into a single vial with standard cornmeal food. Every 24 hours, developmental stages were scored by tracheal morphology as previously described<sup>16</sup>.

**Fluorescence analysis of cholesterol distribution by 22-NBD-cholesterol.** To assess the incorporation of cholesterol and to visualise its distribution, we conducted *in vitro* incubation of the brain-ring gland complexes dissected from third instar larvae with 22-(N-(7-Nitrobenz-2-oxa-1,3-diazol-4-yl)amino)-23,24-bisnor-5-cholen-3 $\beta$ -ol (22-NBD-cholesterol; Life Technologies). 22-NBD-cholesterol was dissolved in 100% ethanol at a 2 mM concentration for a stock solution. To avoid the lethality of *nobo* RNAi at the earlier larval stages, we utilised the *GAL80<sup>ts</sup>* technique<sup>65</sup> to conditionally suppress *GAL4* transcriptional activity during first and second instar larval development. In this experiment, control (*w<sup>1118</sup>*; *UAS-dicer2/+*; *phm-GAL4#22 tubP-GAL80<sup>ts/+</sup>*) and conditional *nobo* RNAi flies (*w<sup>1118</sup>*; *UAS-dicer2/UAS-nobo-IR*; *phm-GAL4#22 tubP-GAL80<sup>ts/+</sup>*) were used. The first instar larvae were transferred into standard cornmeal food and reared at 21°C for 2 days. After 2 days, larvae were then reared at 25°C for an additional 3 days, allowing the larvae to reach the third instar stage. The third instar larvae were dissected in PBS, and the brain-ring gland complexes were transferred into Schneider's *Drosophila* Medium (Life Technologies) containing 10% fetal bovine serum, 100 U/ml penicillin (Wako) and 100  $\mu$ g/ml Streptomycin (Wako). After an incubation at 25°C for 10 min, the medium was replaced with a fresh medium containing 0.5% 22-NBD-cholesterol stock solution, which achieved a 10  $\mu$ M 22-NBD-cholesterol with 0.5% final ethanol concentration. Then, tissues were incubated at 25°C for 6 hours in a dark condition. Tissues were washed with PBS twice and mounted. A 488 nm laser was used for excitation of 22-NBD-cholesterol fluorescence, and fluorescence emission was selected by a 490–555 nm-band pass filter. Fluorescence images were obtained with an LSM 700 laser-scanning confocal microscope (Zeiss).

**A mass-spectrometric quantification of 20E and sterols.** For the measurement of 20E in whole bodies of control (*w<sup>1118</sup>*; *UAS-dicer2/+*; *UAS-phm-GAL4#22/+*) and *nobo* RNAi flies (*w<sup>1118</sup>*; *UAS-dicer2/UAS-nobo-IR*; *UAS-phm-GAL4#22/+*), the second instar larvae (56–64 hours AEL) of each genotype were collected. Then the wet weight of each sample was measured, and the samples were frozen with liquid nitrogen and stored at -80°C until measurement. For the measurement of sterol levels in the RG, the RG samples from the control and *nobo* RNAi larvae were collected as described above in "Fluorescence analysis of cholesterol distribution by 22-NBD-cholesterol". Ten ring glands were collected from the third instar larvae and then transferred into a single glass vial on dry ice. All samples were stored at -80°C until measurement. For each genotype, 10 independent samples, each containing 10 ring glands, were used for the analysis. Extraction of steroids, HPLC fractionation and mass-spectrometric analyses were previously described<sup>66,67</sup>, except a minor modification of the sterol quantification and the mobile phase conditions (run time: 0–12 min, acetonitrile isocratic, flow rate: 300  $\mu$ l/min). In the mass-spectrometric analyses, the exact quantification range was 0.1221–31.25 ng/mL. In this experimental condition, a limit of the quantification of 20E was 0.916 pg of 20E/mg of wet weight sample.

- Spindler, K. D. *et al.* Ecdysteroid hormone action. *Cell Mol Life Sci* **66**, 3837–3850 (2009).
- Yamanaka, N., Rewitz, K. F. & O'Connor, M. B. Ecdysone control of developmental transitions: lessons from *Drosophila* research. *Annu Rev Entomol* **58**, 497–516 (2013).
- Gilbert, L. I., Rybczynski, R. & Warren, J. T. Control and biochemical nature of the ecdysteroidogenic pathway. *Annu Rev Entomol* **47**, 883–916 (2002).
- Niwa, Y. S. & Niwa, R. Neural control of steroid hormone biosynthesis during development in the fruit fly *Drosophila melanogaster*. *Genes Genet. Syst.* **89**, 27–34 (2014).
- Enzymes for ecdysteroid biosynthesis: Their biological functions in insects and beyond. *Biosci Biotechnol Biochem* **78**, 1283–1292 (2014).
- Rewitz, K. F., Rybczynski, R., Warren, J. T. & Gilbert, L. I. The Halloween genes code for cytochrome P450 enzymes mediating synthesis of the insect moulting hormone. *Biochem Soc Trans* **34**, 1256–1260 (2006).
- Niwa, R. *et al.* CYP306A1, a cytochrome P450 enzyme, is essential for ecdysteroid biosynthesis in the prothoracic glands of *Bombyx* and *Drosophila*. *J. Biol. Chem.* **279**, 35942–35949 (2004).
- Yamanaka, N. *et al.* Identification of a novel prothoracicostatic hormone and its receptor in the silkworm *Bombyx mori*. *J. Biol. Chem.* **280**, 14684–14690 (2005).
- Niwa, R. *et al.* The ecdysteroidogenic P450 Cyp302a1/disembodied from the silkworm, *Bombyx mori*, is transcriptionally regulated by prothoracicotropic hormone. *Insect Mol Biol* **14**, 563–571 (2005).
- Namiki, T. *et al.* Cytochrome P450 CYP307A1/Spook: a regulator for ecdysone synthesis in insects. *Biochem Biophys Res Commun* **337**, 367–374 (2005).

- Yoshiyama, T., Namiki, T., Mita, K., Kataoka, H. & Niwa, R. Neverland is an evolutionally conserved Rieske-domain protein that is essential for ecdysone synthesis and insect growth. *Development* **133**, 2565–2574 (2006).
- Namiki, T. *et al.* A basic-HLH transcription factor, HLH54F, is highly expressed in the prothoracic gland in the silkworm *Bombyx mori* and the fruit fly *Drosophila melanogaster*. *Biosci Biotechnol Biochem* **73**, 762–765 (2009).
- Niwa, R. *et al.* Expressions of the cytochrome P450 monooxygenase gene *Cyp4g1* and its homolog in the prothoracic glands of the fruit fly *Drosophila melanogaster* (Diptera: Drosophilidae) and the silkworm *Bombyx mori* (Lepidoptera: Bombycidae) - Springer. *Appl Entomol Zool* **46**, 533–543 (2011).
- Saisawang, C., Wongsantichon, J. & Ketterman, A. J. A preliminary characterization of the cytosolic glutathione transferase proteome from *Drosophila melanogaster*. *Biochem J* **442**, 181–190 (2012).
- Maróy, P., Kaufmann, G. & Dübendorfer, A. Embryonic ecdysteroids of *Drosophila melanogaster*. *J Insect Physiol* **34**, 633–637 (1988).
- Niwa, R. *et al.* Non-moulting glossy/shroud encodes a short-chain dehydrogenase/reductase that functions in the 'Black Box' of the ecdysteroid biosynthesis pathway. *Development* **137**, 1991–1999 (2010).
- Warren, J. T. *et al.* Phantom encodes the 25-hydroxylase of *Drosophila melanogaster* and *Bombyx mori*: a P450 enzyme critical in ecdysone biosynthesis. *Insect Biochem Mol Biol* **34**, 991–1010 (2004).
- Ono, H. *et al.* Spook and Spookier code for stage-specific components of the ecdysone biosynthetic pathway in Diptera. *Dev. Biol.* **298**, 555–570 (2006).
- Yamanaka, N. *et al.* Differential regulation of ecdysteroidogenic P450 gene expression in the silkworm, *Bombyx mori*. *Biosci Biotechnol Biochem* **71**, 2808–2814 (2007).
- McBrayer, Z. *et al.* Prothoracicotropic hormone regulates developmental timing and body size in *Drosophila*. *Dev Cell* **13**, 857–871 (2007).
- Rewitz, K. F., Yamanaka, N., Gilbert, L. I. & O'Connor, M. B. The insect neuropeptide PTTH activates receptor tyrosine kinase torso to initiate metamorphosis. *Science* **326**, 1403–1405 (2009).
- Nüsslein-Volhard, C. & Wieschaus, E. Mutations affecting the pattern of the larval cuticle in *Drosophila melanogaster* I. Zygotic loci on the second chromosome. *Roux's Arch. Dev. Biol.* **193**, 267–282 (1984).
- Chávez, V. M. *et al.* The *Drosophila* disembodied gene controls late embryonic morphogenesis and codes for a cytochrome P450 enzyme that regulates embryonic ecdysone levels. *Development* **127**, 4115–4126 (2000).
- Rong, Y. S. & Golic, K. G. Gene targeting by homologous recombination in *Drosophila*. *Genetics* **288**, 2013–2018 (2000).
- Radford, S. J., Goley, E., Baxter, K., McMahan, S. & Sekelsky, J. *Drosophila* ERCC1 is required for a subset of MEI-9-dependent meiotic crossovers. *Genetics* **170**, 1737–1745 (2005).
- Kennerdell, J. R. & Carthew, R. W. Heritable gene silencing in *Drosophila* using double-stranded RNA. *Nat Biotechnol* **18**, 896–898 (2000).
- Yoshiyama-Yanagawa, T. *et al.* The conserved Rieske oxygenase DAF-36/ Neverland is a novel cholesterol-metabolizing enzyme. *J. Biol. Chem.* **286**, 25756–25762 (2011).
- Niwa, R. & Niwa, Y. S. The Fruit Fly *Drosophila melanogaster* as a Model System to Study Cholesterol Metabolism and Homeostasis. *Cholesterol* **2011**, 176802 (2011).
- Gimpl, G. Cholesterol-protein interaction: methods and cholesterol reporter molecules. *Subcell. Biochem.* **51**, 1–45 (2010).
- Friedman, R. Genomic organization of the glutathione S-transferase family in insects. *Mol Phylogenet Evol* **61**, 924–932 (2011).
- Clark, A. G. *et al.* Evolution of genes and genomes on the *Drosophila* phylogeny. *Nature* **450**, 203–218 (2007).
- Yu, Q. *et al.* Identification, genomic organization and expression pattern of glutathione S-transferase in the silkworm, *Bombyx mori*. *Insect Biochem Mol Biol* **38**, 1158–1164 (2008).
- Ayres, C. *et al.* Comparative genomics of the anopheline glutathione S-transferase epsilon cluster. *PLoS ONE* **6**, e29237 (2010).
- Johansson, A. S. & Mannervik, B. Human glutathione transferase A3-3, a highly efficient catalyst of double-bond isomerization in the biosynthetic pathway of steroid hormones. *J. Biol. Chem.* **276**, 33061–33065 (2001).
- Raffalli-Mathieu, F., Orre, C., Stridsberg, M., Hansson Edalat, M. & Mannervik, B. Targeting human glutathione transferase A3-3 attenuates progesterone production in human steroidogenic cells. *Biochem J* **414**, 103–109 (2008).
- Tars, K., Olin, B. & Mannervik, B. Structural basis for featuring of steroid isomerase activity in alpha class glutathione transferases. *J Mol Biol* **397**, 332–340 (2010).
- Fedulova, N., Raffalli-Mathieu, F. & Mannervik, B. Porcine glutathione transferase Alpha 2-2 is a human GST A3-3 analogue that catalyses steroid double-bond isomerization. *Biochem J* **431**, 159–167 (2010).
- Kim, J. *et al.* Identification and characteristics of the structural gene for the *Drosophila* eye colour mutant sepia, encoding PDA synthase, a member of the omega class glutathione S-transferases. *Biochem J* **398**, 451–460 (2006).
- Kim, K. K., Kim, S.-H. S., Kim, J. J., Kim, H. H. & Yim, J. J. Glutathione S-transferase omega 1 activity is sufficient to suppress neurodegeneration in a *Drosophila* model of Parkinson disease. *J. Biol. Chem.* **287**, 6628–6641 (2012).
- Chanut-Delalande, H. *et al.* Pri peptides are mediators of ecdysone for the temporal control of development. *Nat Cell Biol* DOI:10.1038/ncb3052 (2014) in press.



41. Prova, C. Glutathione transferases in the genomics era: new insights and perspectives. *Biomol Eng* **23**, 149–169 (2006).
42. Tew, K. D. & Townsend, D. M. Glutathione-S-transferases as determinants of cell survival and death. *Antioxid. Redox Signal.* **17**, 1728–1737 (2012).
43. Enayati, A. A., Ranson, H. & Hemingway, J. Insect glutathione transferases and insecticide resistance. *Insect Mol Biol* **14**, 3–8 (2005).
44. Sun, X.-Q. *et al.* Glutathione S-transferase of brown planthoppers (*Nilaparvata lugens*) is essential for their adaptation to gramine-containing host plants. *PLoS ONE* **8**, e64026 (2013).
45. Shabab, M., Khan, S. A., Vogel, H., Heckel, D. G. & Boland, W. OPDA isomerase GST16 is involved in phytohormone detoxification and insect development. *FEBS J* **281**, 2769–2783 (2014).
46. Laborde, E. Glutathione transferases as mediators of signaling pathways involved in cell proliferation and cell death. *Cell Death Differ* **17**, 1373–1380 (2010).
47. Tew, K. D. *et al.* The role of glutathione S-transferase P in signaling pathways and S-glutathionylation in cancer. *Free Radic Biol Med* **51**, 299–313 (2011).
48. Raffalli-Mathieu, F. & Mannervik, B. Human Glutathione Transferase A3-3 Active as Steroid Double-Bond Isomerase. *Methods Enzymol* **401**, 265–278 (2005).
49. Svoboda, J. A., Kaplanis, J. N., Robbins, W. E. & Thompson, M. J. Recent developments in insect steroid metabolism. *Annu Rev Entomol* **20**, 205–220 (1975).
50. Huang, X., Suyama, K., Buchanan, J., Zhu, A. J. & Scott, M. P. A *Drosophila* model of the Niemann-Pick type C lysosome storage disease: *dncp1a* is required for molting and sterol homeostasis. *Development* **132**, 5115–5124 (2005).
51. Fluegel, M. L., Parker, T. J. & Pallanck, L. J. Mutations of a *Drosophila* NPC1 gene confer sterol and ecdysone metabolic defects. *Genetics* **172**, 185–196 (2006).
52. Huang, X., Warren, J. T., Buchanan, J., Gilbert, L. I. & Scott, M. P. *Drosophila* Niemann-Pick Type C-2 genes control sterol homeostasis and steroid biosynthesis: a model of human neurodegenerative disease. *Development* **134**, 3733–3742 (2007).
53. Rosenbaum, A. I. & Maxfield, F. R. Niemann-Pick type C disease: molecular mechanisms and potential therapeutic approaches. *J Neurochem* **116**, 789–795 (2011).
54. Ohkama-Ohtsu, N. *et al.* 12-oxo-phytyldienoic acid-glutathione conjugate is transported into the vacuole in Arabidopsis. *Plant Cell Physiol* **52**, 205–209 (2011).
55. Talamillo, A. *et al.* Scavenger Receptors Mediate the Role of SUMO and Ftz-f1 in *Drosophila* Steroidogenesis. *PLoS Genet* **9**, e1003473 (2013).
56. Ou, Q., Magico, A. & King-Jones, K. Nuclear receptor DHR4 controls the timing of steroid hormone pulses during *Drosophila* development. *PLoS Biol* **9**, e1001160 (2011).
57. Rewitz, K. F., Styryshave, B., Løbner-Olsen, A. & Andersen, O. Marine invertebrate cytochrome P450: emerging insights from vertebrate and insects analogies. *Comp Biochem Physiol C Toxicol Pharmacol* **143**, 363–381 (2006).
58. Rewitz, K. F., O'Connor, M. B. & Gilbert, L. I. Molecular evolution of the insect Halloween family of cytochrome P450s: phylogeny, gene organization and functional conservation. *Insect Biochem Mol Biol* **37**, 741–753 (2007).
59. Markstein, M., Pitsouli, C., Villalta, C., Celniker, S. E. & Perrimon, N. Exploiting position effects and the gypsy retrovirus insulator to engineer precisely expressed transgenes. *Nat Genet* **40**, 476–483 (2008).
60. Foley, K. P., Leonard, M. W. & Engel, J. D. Quantitation of RNA using the polymerase chain reaction. *Trends Genet* **9**, 380–385 (1993).
61. Shimada, Y., Burn, K. M., Niwa, R. & Cooley, L. Reversible response of protein localization and microtubule organization to nutrient stress during *Drosophila* early oogenesis. *Dev. Biol.* **355**, 250–262 (2011).
62. Brand, A. H. & Perrimon, N. Targeted Gene-Expression as a Means of Altering Cell Fates and Generating Dominant Phenotypes. *Development* **118**, 401–415 (1993).
63. Matsuo, T., Sugaya, S., Yasukawa, J., Aigaki, T. & Fuyama, Y. Odorant-binding proteins OBP57d and OBP57e affect taste perception and host-plant preference in *Drosophila sechellia*. *PLoS Biol* **5**, e118 (2007).
64. Wieschaus, E. & Nüsslein-Volhard, C. in *Drosophila: A Practical Approach* (Roberts, D. B.) 179–214 (Oxford University Press, 1998).
65. McGuire, S. E., Le, P. T., Osborn, A. J., Matsumoto, K. & Davis, R. L. Spatiotemporal rescue of memory dysfunction in *Drosophila*. *Science* **302**, 1765–1768 (2003).
66. Hikiba, J. *et al.* Simultaneous quantification of individual intermediate steroids in silkworm ecdysone biosynthesis by liquid chromatography-tandem mass spectrometry with multiple reaction monitoring. *J. Chromatogr. B Analyt. Technol. Biomed. Life Sci.* **915–916**, 52–56 (2013).
67. Igarashi, F. *et al.* A highly specific and sensitive quantification analysis of the sterols in silkworm larvae by high performance liquid chromatography-atmospheric pressure chemical ionization-tandem mass spectrometry. *Anal Biochem* **419**, 123–132 (2011).

## Acknowledgments

We are grateful to Drs. Takashi Matsuo, Michael B. O'Connor, Ryosuke L. Ohniwa, and Jeongbin Yim and the Bloomington *Drosophila* Stock Center, the *Drosophila* Genetic Resource Center in Kyoto, the Vienna *Drosophila* RNAi Center and the Developmental Studies Hybridoma Bank for stocks and reagents. We also thank Dr. Satomi Takeo for helpful advice for creating knock-out strains; Drs. Yuko Shimada-Niwa and DeMar Taylor for critical reading of the manuscript; and Drs. François Payre and Yuji Kageyama for a helpful and constructive discussion on this work. S.E. was a recipient of a fellowship from the Japan Society for the Promotion of Science. This work was supported in part by Special Coordination Funds for Promoting Science and Technology from the Ministry of Education, Culture, Sports, Science and Technology of the Japanese government. This work was also supported by JSPS KAKENHI Grant Number 25712010 and MEXT KAKENHI Grant Number 23116701 on Innovative Areas 'Regulatory Mechanism of Gamete Stem Cells' to R.N. and by JSPS KAKENHI Grant Number 25252023 to H.K.

## Author contributions

S.E. and R.N. designed the study; S.E., T.A., F.I., M.I., T.S. and R.N. performed the experiments; S.E., F.I., M.I., H.K., T.S. and R.N. contributed and developed reagents; S.E., T.A., F.I., M.I., T.S. and R.N. analysed the data; and S.E. and R.N. wrote the paper.

## Additional information

**Supplementary information** accompanies this paper at <http://www.nature.com/scientificreports>

**Competing financial interests:** The authors declare no competing financial interests.

**How to cite this article:** Enya, S. *et al.* A Halloween gene *noppera-bo* encodes a glutathione S-transferase essential for ecdysteroid biosynthesis via regulating the behaviour of cholesterol in *Drosophila*. *Sci. Rep.* **4**, 6586; DOI:10.1038/srep06586 (2014).



This work is licensed under a Creative Commons Attribution-NonCommercial-ShareAlike 4.0 International License. The images or other third party material in this article are included in the article's Creative Commons license, unless indicated otherwise in the credit line; if the material is not included under the Creative Commons license, users will need to obtain permission from the license holder in order to reproduce the material. To view a copy of this license, visit <http://creativecommons.org/licenses/by-nc-sa/4.0/>